European Journal of Medicinal Chemistry 235 (2022) 114258

Contents lists available at ScienceDirect

European Journal of Medicinal Chemistry

journal homepage: http://www.elsevier.com/locate/ejmech

HR1405-01, a Safe intravenous NSAID with superior anti-inflammatory and analgesic activities in preclinical trials

Hai Ye [a, b, e], Tian Lv [b], Tao Min [b], Di Mao [d], Xingran Chen [b], Boxiang Ding [b], Can Zhang [a, c, *]

[a] State Key Laboratory of Natural Medicines, Jiangsu Key Laboratory of Drug Discovery for Metabolic Diseases, Jiangsu Key Laboratory of Drug Screening, China Pharmaceutical University, Nanjing, 210009, PR China
[b] Nanjing Heron Pharmaceutical Science and Technology Co., Ltd., Nanjing, 211112, PR China
[c] Center of Advanced Pharmaceuticals and Biomaterials, China Pharmaceutical University, Nanjing, 210009, PR China
[d] School of Pharmacy, Jiangsu University, Zhenjiang, 212013, PR China
[e] Jiangsu Hot Melt Extrusion Engineering Research Center, Nanjing, 211112, PR China

ARTICLE INFO

Article history:
Received 22 December 2021
Received in revised form
3 March 2022
Accepted 3 March 2022
Available online 18 March 2022

ABSTRACT

Combinational utilization of intravenous non-steroidal anti-inflammatory drugs (NSAIDs) with opium analgesic is an effective alternative modality for pain control after surgery. This regimen is known for reducing the risk of addiction induced by opium analgesic. However, current intravenous NSAIDs have solubility problems, limiting their clinical applications. Although loxoprofen exhibits strong anti-inflammatory and analgesic activities with relatively low ulcerogenicity, its relatively low bioavailability makes it not an ideal drug candidate for intravenous injection. We selected the bioactive metabolite (**6**) of loxoprofen as a candidate and developed a new intravenous NSAID, **HR1405–01**. This metabolite exhibited significantly stronger anti-inflammatory and analgesic activities than parecoxib sodium injection or ibuprofen injection. The excellent potency and solubility of **HR1405–01** allowed the avoidance of utilization of cosolvent in the formulation, resulting in fewer side effects and a better safety profile. Therefore, **HR1405–01** might be a promising candidate for the development of a new intravenous NSAID.

1. Introduction

Non-steroidal anti-inflammatory drugs (NSAIDs) are one of the most widely used drugs for suppressing fever and pain. NSAIDs exert their anti-inflammatory activities through inhibiting cyclooxygenase (COX), an enzyme that is essential for converting arachidonic acid (AA) into inflammation inducers such as prostaglandins (PGs) and thromboxane A2 (TXA2). Two main subtypes of COX including COX-1 and COX-2 have been identified [1,2]. COX-1 is a predominantly constitutive enzyme that is widely expressed in most tissues, playing an important role in human tissue homeostasis. Unlike COX-1, COX-2 is an inducible enzyme, which can be induced by stimuli such as lipopolysaccharides (LPS) and interleukin 2 (IL-2).

Conventional NSAIDs inhibit both COX-1 and COX-2 [3,4]. Lack of selectivity for COX-2 is believed to be the reason for their side effects of gastrointestinal (GI) injury and inhibition of platelet function [5]. Selective COX-2 inhibitors have been developed to reduce GI injury [6–8]. However, it was reported that selective COX-2 inhibition increased the risk of serious cardiovascular side effects [9–12]. Such serious side effects resulted in the withdrawal of the three selective COX-2 inhibitors (rofecoxib, lumiracoxib, and Valdecoxib) from the market. Therefore, focusing on non-selective COX inhibitors might be a more rational and effective way to develop new NSAIDs.

In recent years, intravenous NSAIDs have gained attention. Combinational utilization of intravenous ibuprofen with morphine has been reported to reduce the total use of morphine, resulting in less risk of addiction [13]. Until now, eight intravenous NSAIDs, including ibuprofen injection, parecoxib sodium injection, diclofenac sodium injection, ketorolac tromethamine salt injection, flurbiprofen axetil injection, lornoxicam injection, meloxicam injection, and indomethacin sodium injection, have been approved for clinical use. However, their clinical applications are limited by

* Corresponding author. State Key Laboratory of Natural Medicines, Jiangsu Key Laboratory of Drug Discovery for Metabolic Diseases, Jiangsu Key Laboratory of Drug Screening, China Pharmaceutical University, Nanjing, 210009, PR China.
E-mail address: zhangcan@cpu.edu.cn (C. Zhang).

https://doi.org/10.1016/j.ejmech.2022.114258
0223-5234/

the poor solubilities and the side effects induced by the cosolvents. Therefore, it is urgent to develop new potent intravenous NSAIDs with high solubility.

Loxoprofen sodium (Fig. 1), an oral phenylpropionate NSAID produced by Sankyo pharma, was approved in Brazil, Mexico, and Japan for the treatment of inflammatory diseases and postoperative analgesia. In January 2006, the transdermal patch of loxoprofen was approved for clinical use in Japan [14]. Loxoprofen exhibits strong anti-inflammatory and analgesic activities with relatively low ulcerogenicity. Nevertheless, as an oral administrative prodrug, loxoprofen is not an ideal candidate for the development of intravenous injection due to its low conversion rate (22% in the liver), high dosage (a mixture of four stereoisomers), and poor solubility [15].

Loxoprofen is converted into eight metabolic products, which are optical isomers, by aldehydeketone reductases and carbonyl reductases after absorption in the gastrointestinal tract (Fig. 1). The structures of the eight optical isomers are shown in Fig. 1. Among them, only loxoprofenol-SRS (**6**) acts as the active metabolite [15]. Loxoprofenol-SRS (**6**) was reported as a potent and nonselective inhibitor for COX-1 and COX-2 in both enzymatic assays (IC_{50} for COX-1: 0.5 ± 0.08 μM; IC_{50} for COX-2: 0.39 ± 0.05 μM) and human whole blood assays (IC_{50} for COX-1: 0.28 ± 0.08 μM; IC_{50} for COX-2: 0.3 ± 0.05 μM) [16]. However, a recent study reported that loxoprofenol-SRS (**6**) exhibited moderate selectivity for human recombinant COX-2 (IC_{50} for COX-1: 1.47 μM; IC_{50} for COX-2: 0.026 μM) [17]. It was reported that pharmacokinetics of loxoprofen was independent of the routes of administration, and the conversion of loxoprofen into the metabolites occurred both in the liver and extrahepatic tissue(s) [15]. Such metabolic characteristics suggested that loxoprofen might exhibit more potent anti-inflammatory and analgesic activity through intravenous injection than oral administration. Consequently, we hypothesized that loxoprofenol-SRS (**6**), the active metabolite, might be a promising candidate for the development of a new intravenous NSAID.

Herein, we selected loxoprofenol-SRS (**6**) and developed a new intravenous NSAID **HR1405–01**. To conduct the synthesis and preclinical studies of **HR1405–01**, loxoprofenol-SRS (**6**, Scheme 1), and its seven isomers (**PY2**-**PY8**, Scheme 2, and Scheme 3) were synthesized with the optimized method [18]. Such a method allowed us to produce the loxoprofenol-SRS (**6**) with a large scale (>2 kg), high optical purity, and a high yield (20.6%) (Scheme 1). The first synthesis of the seven isomers (**PY2**-**PY8**) also allowed us to conduct a full evaluation of the metabolism of **HR1405–01** *in vivo*.

2. Results and discussion

2.1. Synthetic routes

The synthesis of loxoprofenol-SRS (**6**) was previously reported [18]. However, such a method was not suitable for the preparation of **6** in the pharmaceutical process because of the use of strong unstable inorganic acid (HO_3SONO), strong reaction exotherm, and the following problem of racemation of 2-C (Fig. S1). To solve the problems, we re-designed the synthetic route which allowed us to remove the use of strong inorganic acid and prepare loxoprofenol-SRS (**6**) with a large scale (>2 kg) and high optical purity (enantiomeric excess (ee) > 98%). The synthetic route of **HR1405–01** was depicted in Scheme 1. The (*S*)-(−)-1-phenylethylamine was mixed with loxoprofen in ethyl acetate and the precipitate was collected and recrystallized two times with toluene/MeOH to afford compound **1** (e.e>98%), which was then acidified with 2 N HCl to produce **2**. Compound **2** was reduced by $NaBH_4$ to produce the *cis*-alcohol **3** and *trans*-alcohol **4**, which were simply purified by silica gel column chromatography. The reaction of **4** with vinyl acetate in the presence of Amano lipase PS (Amano PS) generated **5** and **6** [19,20], which were easily separated by silica gel column chromatography. The absolute configuration of **6** was determined by the single-crystal X-ray diffraction (Fig. 2). Compound **6** was finally treated with tromethamine in EtOH/ethyl acetate to afford the target compound **HR1405–01**. The structure of **HR1405–01** was characterized by ultraviolet spectroscopy (UV), infrared spectroscopy (IR), high-resolution mass spectrometry (HRMS), nuclear magnetic resonance spectroscopy (NMR), differential scanning calorimetry (DSC), thermogravimetric analysis (TG), optical rotation, and melting point (m.p.). The absolute configuration of

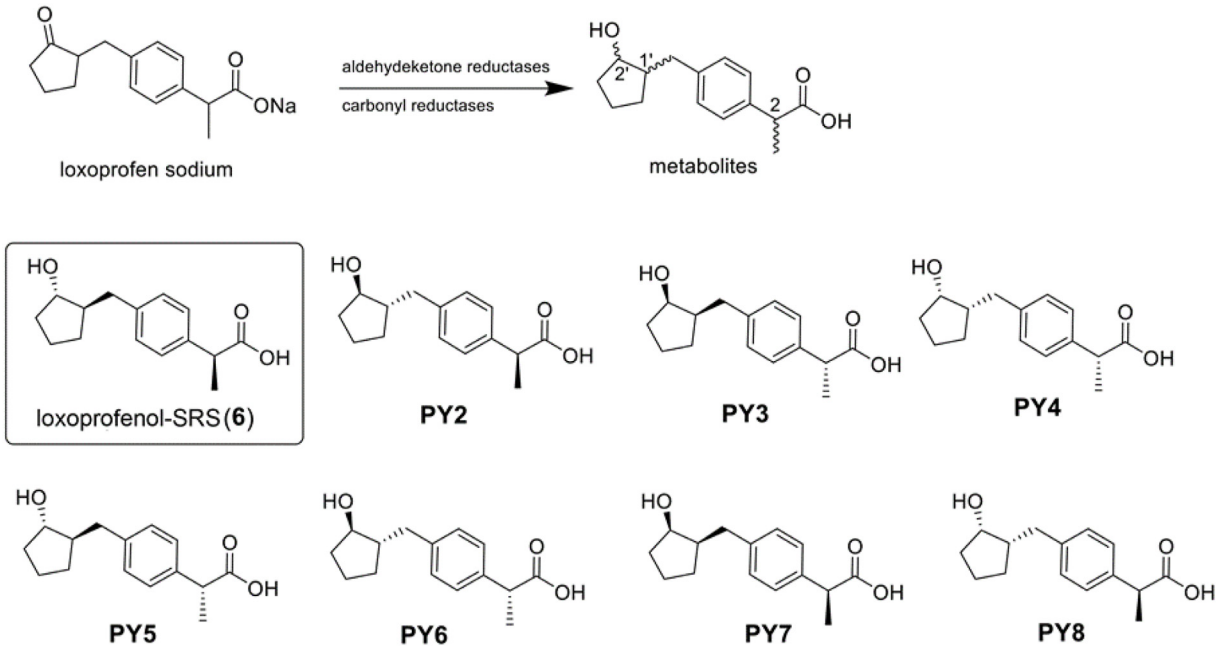

Fig. 1. Enzymatic metabolism of loxoprofen sodium and chemical structures of the active metabolite loxoprofenol-SRS (**6**) and the seven inactive metabolites (**PY2**-**PY8**).

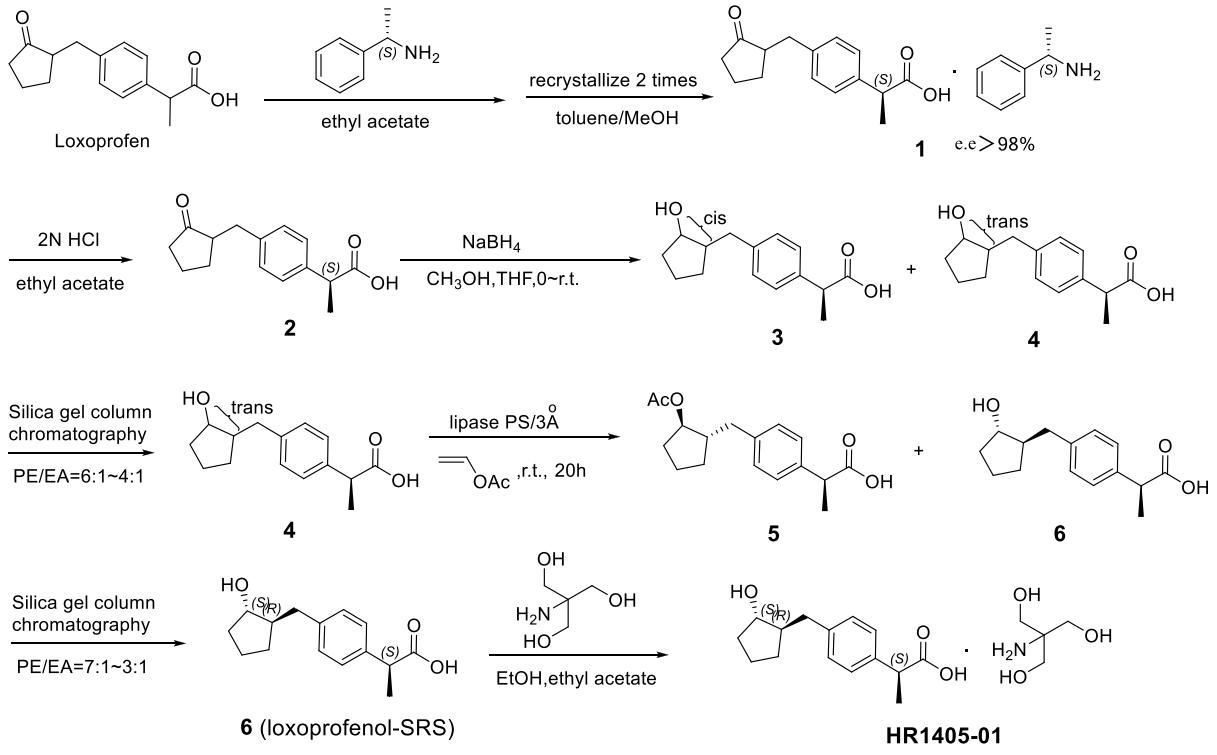

Scheme 1. Synthetic route of **6** (loxoprofenol-SRS) and **HR1405−01**.

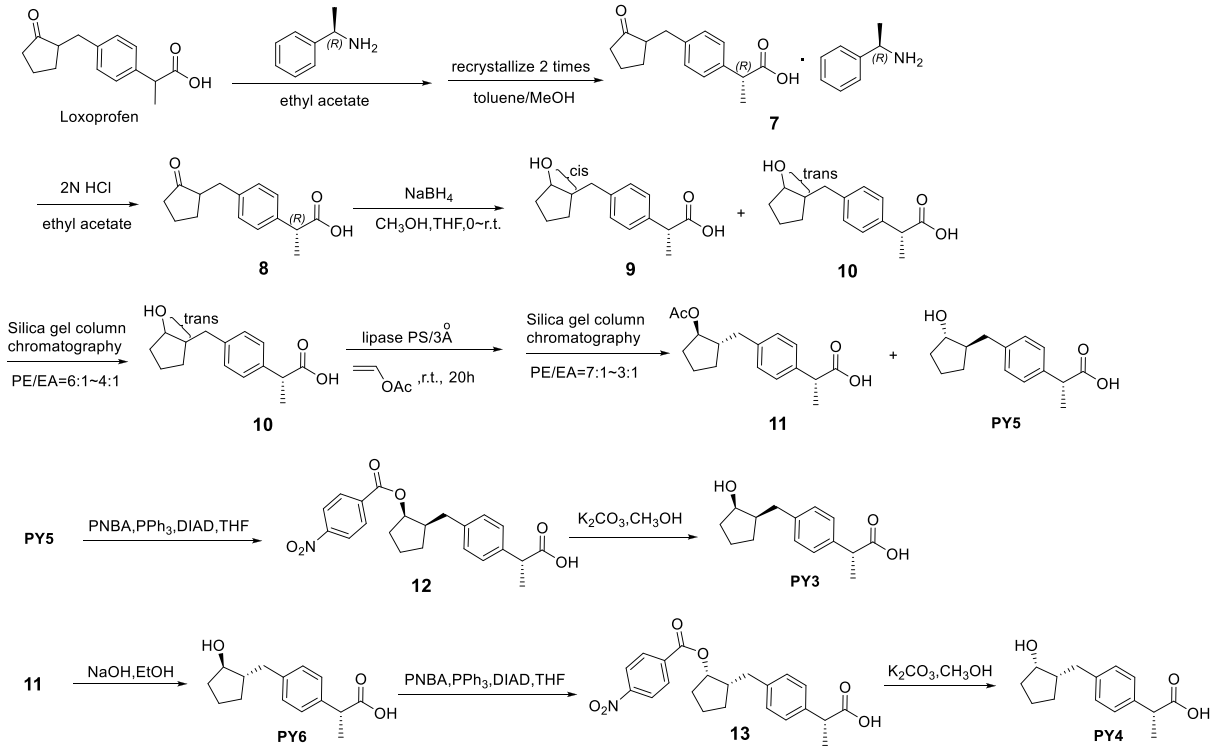

Scheme 2. Synthetic route of **PY3-PY6**.

HR1405−01 was determined on the basis of the absolute configuration of compound **6**.

The synthetic routes of **PY2-PY8** were depicted in Scheme 2 and Scheme 3. Briefly, **PY5** was synthesized with a similar synthetic route of **6** by replacing (*S*)-(−)-1-phenylethylamine with (*R*)-(+)-1-phenylethylamine in the first step. **PY3** was obtained from **PY5** with the chiral inversion of 2′-C via the classic Mitsunobu Reactions. The reaction of **PY5** with *p*-nitrobenzoic acid (PNBA) in the

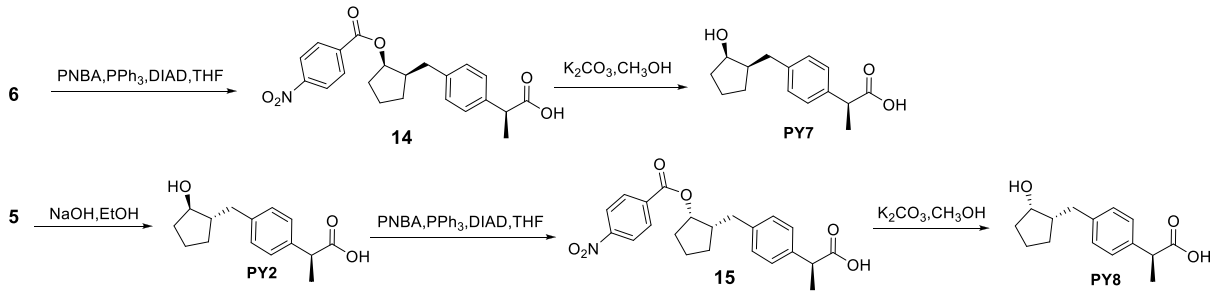

Scheme 3. Synthetic route of **PY2**, **PY7,** and **PY8**.

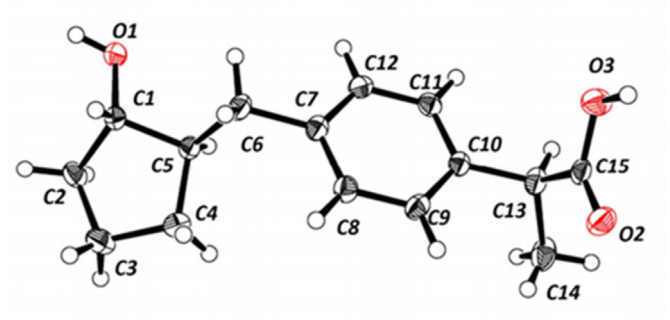

Fig. 2. Thermal vibration ellipsoid of **6** by X-ray diffraction.

presence of triphenylphosphine (PPh_3) and diisopropyl azodicarboxylate (DIAD) generated intermediate **12**, which was further hydrolyzed with K_2CO_3 in CH_3OH to produce **PY3**. Intermediate **5** and **11** were easily hydrolyzed by NaOH to generate **PY2** and **PY6**, respectively, without affecting the chirality of 2′-C. **PY4**, **PY7**, and **PY8** were prepared from **PY6**, **6,** and **PY2** via Mitsunobu Reactions, respectively.

The structures of **PY2-PY8** were characterized by HRMS, NMR, DSC, TG, optical rotation, melting point, and their absolute configurations were determined on the basis of the absolute configuration of compound **6**. The NMR spectra (^{1}H and ^{13}C) of the *trans*-isomers (**6**, **PY2**, **PY5**, and **PY6**) were almost the same and so were the *cis*-isomers (**PY3**, **PY4**, **PY7**, **PY8**). The differences between the *trans*-isomers and the *cis*-isomers could be observed at the chemical shifts of 2-H and 2′-H in ^{1}H NMR and the chemical shifts of benzylic carbon in ^{13}C NMR (Fig. S2)

2.2. Anti-inflammatory and analgesic activities of *HR1405–01* in vivo

Initially, the water solubility of **HR1405–01** was investigated. **HR1405–01** exhibited excellent water solubility (176.1 mg/mL) which was much better than that of the two positive controls, parecoxib sodium injection (18 mg/mL in H_2O at pH 7.8, the data was obtained from Dynastat ePar Scientific Discussion. https://www.ema.europa.eu/en/documents/scientific-discussion/dynastat-epar-scientific-discussion_en.pdf.) and ibuprofen injection (0.0219 mg/mL in H_2O, the data was obtained from Drug Bank. https://go.drugbank.com/drugs/DB01050). The great solubility encouraged us to further validate the anti-inflammatory and analgesic activities of **HR1405–01** *in vivo*. Four classic anti-inflammatory and analgesic assays, including the writhing test, carrageenan-induced arthritic inflammation assay, carrageenan-induced mechanical hyperalgesia assay, and the formalin test were performed. In the writhing test, **HR1405–01** injection exhibited great analgesic activity (ED_{50}: 0.43 mg/kg), which was more than 10 times stronger than that of parecoxib sodium injection (ED_{50}: 15.72 mg/kg) or ibuprofen injection (ED_{50}: 5.00 mg/kg) (Table 1). Such strong analgesic activity of **HR1405–01** was also observed in the carrageenan-induced mechanical hyperalgesia assay (ED_{50}: 1.28 mg/kg) (Table S1) and formalin test (Table S2). However, in the anti-inflammatory assays, **HR1405–01** didn't perform as well as it did in the analgesic assays. In carrageenan-induced arthritic inflammation assay, the **HR1405–01** showed relatively moderate anti-inflammatory activity (ED_{50}: 8.01 mg/kg), only being 2.83 times stronger than that of parecoxib sodium injection (ED_{50}: 22.67 mg/kg) and 2.62 times stronger than that of ibuprofen injection (ED_{50}: 21.04 mg/kg) (Table S3). Such significant differences between analgesic activities and anti-inflammatory activities were most likely due to the rapid distribution and relatively slow inflammatory elimination effect of **HR1405–01** injection *in vivo*. Taking advantage of the high potency and excellent solubility of **HR1405–01**, we designed the formulation with no use of cosolvent in the preclinical and clinical trials, removing the potential risk of side effects induced by cosolvent. These results collectively suggested that **HR1405–01** might serve as a promising candidate for the development of a new intravenous NSAID.

2.3. Pharmacokinetics of *HR1405–01* after intravenous administration

Subsequently, pharmacokinetic studies of **HR1405–01** after intravenous administration were carried out to investigate its metabolism. The stereochemical conversions of **HR1405–01** into its seven isomers **PY2-PY8** in rat and Beagle dog plasma were investigated as the absolute configuration played a key role in the activity. In the rat plasma, no detectable **PY-2**, **PY-3**, **PY-4,** and **PY-6** were observed. For **PY-5**, **PY-7,** and **PY-8**, the conversions were less than 2%. In the dog plasma, the conversions were slightly stronger than those in the rat plasma. No detectable conversion of **HR1405–01** to **PY-3**, **PY-4,** or **PY-6** was observed. For **PY-2**, **PY-5**, **PY-7,** and **PY-8**, the conversions were from 0.05% to 7.25%. The total chiral conversions were 1.70% (male) and 2.24% (female) in rat plasma, and 5.59% (male) and 9.44% (female) in dog plasma (Fig. 3, Table S4). Strong chirality inversions at all of the three chiral centers (2-C, 1′-C, and 2′-C) were not observed in the metabolism of **HR1405–01** *in vivo*. The results indicated that **HR1405–01** exhibited great stereochemical stability in the plasma of rat and Beagle dog. However, it is noteworthy that the total conversions of **HR1405–01** into its seven isomers (**PY2-PY8**) in Beagle dog plasma (5.59% for male and 9.44% for female) were stronger than those in rat plasma (1.70% for male and 2.24% for female). These observations suggested that **HR1405–01** might exhibit distinct metabolism profile in different species. Further investigation of chiral stability of **HR1405–01** in human plasma might be warranted before its clinical application.

Table 1
HR1405–01 injection reduced 0.6% acetic acid-induced pain (writhing test).

Group	Dose(mg/kg)	Average writhing times within 15 min	Inhibition effect ratios(%)	ED_{50}(mg/kg)	95% confidence interval(mg/kg)
HR1405-01 injection	0 (vehicle)	21.1 ± 16.3	–	0.43	0.178–0.930
	0.13	19.0 ± 12.7	10.0		
	0.25	12.8 ± 6.5	39.3		
	0.50	7.7 ± 5.1	63.5		
	1.00	6.7 ± 13.9	68.2		
Parecoxib sodium injection	0 (vehicle)	26.1 ± 16.3	–	15.72	9.09–26.9
	6.25	22.2 ± 15.3	14.9		
	12.50	13.7 ± 4.4	47.5		
	25.00	10.1 ± 6.6	61.3		
	50.00	2.4 ± 3.3	90.8		
Ibuprofen injection	0 (vehicle)	26.1 ± 16.3	–	5.00	2.55–8.51
	3.13	21.0 ± 12.7	19.5		
	6.25	6.1 ± 3.6	76.6		
	12.50	4.0 ± 4.4	84.7		
	25.00	3.0 ± 4.1	88.5		

Data are given as mean ± standard deviation (SD). n = 10. Physiological saline (0.9% NaCl) was used as a vehicle.

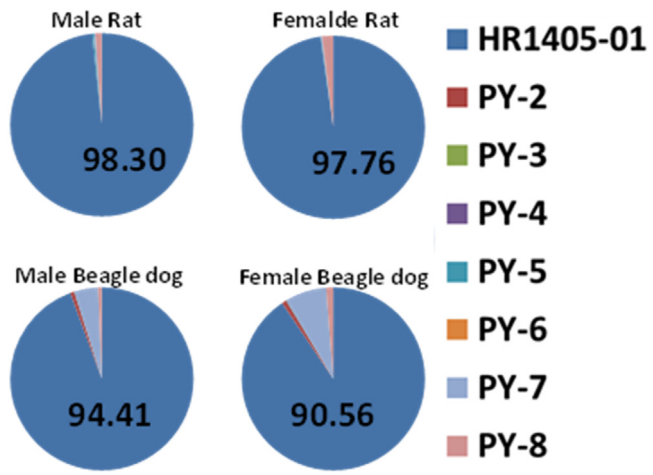

Fig. 3. Percentage conversion (%) of **HR1405–01** to **PY2-PY8** in rat and Beagle dog plasma. **HR1405–01** injection was administered intravenously to SD Rats (male or female) and Beagle dogs (male or female) at 3 mg/kg. After 2 h, the plasma of each animal was extracted and the extract was analyzed by UHPLC-MS/MS, respectively.

NSAIDs have been reported to show strong plasma protein binding rates [21]. The plasma protein binding rates of **HR1405–01** were investigated with the plasma of CD-1 mouse, Sprague-Dawley rat, Beagle dog, Cynomolgus monkey, and human. Three dosages (low dose: 600 ng/ml; middle dose: 3000 ng/ml; high dose: 15,000 ng/ml) were selected and tritium-labeled Taxol (2000 ng/ml) was used as a positive control. As shown in Table S5, **HR1405–01** exhibited strong plasma protein binding rates (>70%) in a non-dose-dependent manner in all species. Among them, the strongest plasma protein binding rates (>95%) were observed in human, suggesting the potential slow release of **HR1405–01** in human plasma after injection.

Subsequently, pharmacokinetic parameters of **HR1405–01** were fully evaluated with rat and Beagle dog. The pharmacokinetic parameters calculated with rat plasma were listed in Table S6 and the Log drug amount vs. time profile of plasma concentration was depicted in Fig. 4. Significant differences for the steady-state volume of distribution (Vss), clearance (CL), and area under the curve (AUC) between female and male rats were observed at the middle (0.8 mg/kg) and high dosage (3 mg/kg). At the dosage of 3 mg/kg, the AUC of **HR1405–01** in the female rat plasma was more than 3 times higher than that in the male rat plasma. On the other hand, the CL of **HR1405–01** in the female rat plasma was more than 3 times slower than that in the male rat plasma. Notably, there was no significant difference in C_{max} between the two genders (Table S6). These results collectively indicated that the rate of clearance of **HR1405–01** in male rats was higher than in female rats (Fig. 4). Surprisingly, in Beagle dog plasma, no significant pharmacokinetic differences between the two genders were observed (Fig. 4, Table S7). The results suggested that **HR1405–01** might exhibit distinct metabolism in different species. Further investigation of the metabolism of **HR1405–01** in human plasma will be needed before clinical application.

2.4. The toxicity test of repeated administrations of *HR1405–01*

To evaluate the safety of **HR1405–01**, repeated-dose toxicity studies in the rats and Beagle dogs were carried out. Three dosages (low dose: 1 mg/kg; middle dose: 3 mg/kg; high dose: 10 mg/kg) were selected to evaluate the toxicity. In rats, after treatment of **HR1405–01** (10 mg/kg), the total numbers of both red blood cells (RBC) and hemoglobin (HGB) exhibited a less than 10% decrease in both genders. Meanwhile, the slight changes in the red cell distribution width (RDW), mean corpuscular hemoglobin concentration (MCHC), and percentage of reticulocyte (Ret %) were observed and there was no significant difference in the other parameters. In the 8th week, all the changes above recovered completely. In Beagle dogs, no significant changes were observed even at the high dosage (10 mg/kg). These results indicated that **HR1405–01** exhibited little effect on the hematologic system.

In addition, a local tolerance study was further carried out to evaluate the safety of **HR1405–01**. A vascular stimulation test (histopathological examination) with young New Zealand white rabbits was performed. The results showed that there was no inflammatory cell infiltration, no necrosis of endothelial cells, or other significant difference after treatment of **HR1405–01**, indicating that **HR1405–01** exhibited good local tolerance (Fig. S3). These results collectively demonstrated that **HR1405–01** exhibited great safety in model animals.

3. Conclusions

In conclusion, we developed a new intravenous NSAID, **HR1405–01**, which was a tromethamine salt of loxoprofenol-SRS. The seven stereoisomers (**PY2-PY8**) of loxoprofenol-SRS were also synthesized as references for the pharmaceutical process and the pharmacokinetics studies of **HR1405–01**. As a new intravenous NSAID candidate, **HR1405–01** exhibited superior anti-inflammatory and analgesic activities, stereochemical stability,

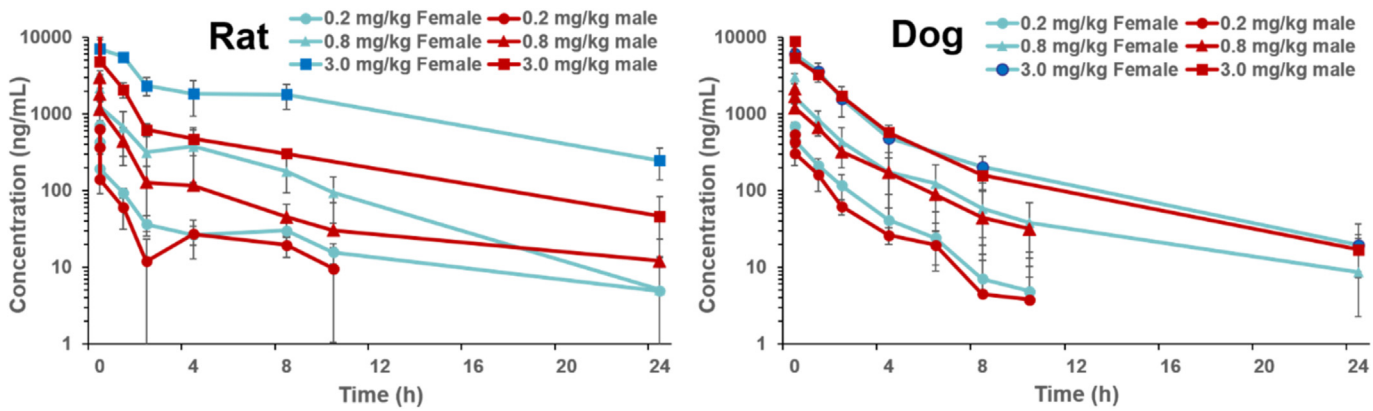

Fig. 4. Log amount-time profiles of **HR1405–01** in rats (left) and Beagle dogs (right) plasma. Each value represents the mean ± SD. n = 6.

and safety in animal studies. The great potency and solubility allowed the avoidance of utilization of cosolvents in the formulation, resulting in less side effects and a better safety profile. Benefiting from its great solubility (176.1 mg/mL), **HR1405–01** injection exhibited a significantly better dosage/solubility ratio than those of the other intravenous NSAIDs in clinical use (Table S8). It was believed that the superior potency, solubility, stereochemical stability, and safety profile made **HR1405–01** injection a promising candidate for clinical application. Indeed, prelimited results of a phase I clinical trial indicated that **HR1405–01** injection exhibited faster peak time (T_{max}) (30 min by intravenous administration vs 60 min by oral administration) and lower effective dose (20 mg for **HR1405–01** vs 60 mg for loxoprofen) than loxoprofen (Fig. S4). The further clinical investigation will be performed in the near future.

4. Experimental section

All reagents and solvents were purchased from commercial suppliers and used as received without further drying or purification. Loxoprofen was purchased from Bejingzhongshuo Co., Ltd. Melting points were determined by DSC. ^{1}H NMR (300 or 500 MHz) and ^{13}C NMR (75 or 125 MHz) spectra were recorded with Bruker Avance 300 and 500 MHz spectrometers at 303 K, using tetramethylsilane as an internal standard. Mass and high-resolution mass spectrometry (HRMS) spectra were obtained on an Agilent Q-TOF 6520 or Waters Synapt G2-S spectrometer. Analytical and preparative thin-layer chromatography was performed on silica gel (200 – 300 mesh) GF/UV 254 plates, and the chromatograms were visualized under UV light at 254 nm. Analytical reversed-phase HPLC (RPLC) was conducted on a Shimadzu Prominence High-Performance Liquid Chromatography (HPLC) system using Innovai ODS-2 column (5 μm, 100 Å, 150 or 250 × 4.60 mm). All compounds are >95% pure by HPLC analysis. HPLC traces of the compounds used *in vivo*, including **HR1405–01** and **PY2-PY8**, are shown in supporting information. Male Sprague-Dawley rats (male: 240.7–318.4 g, female: 218.3–267.5 g) were purchased from Beijing Vital River Laboratory Animal Technology Co., Ltd. ICR mice (18–22 g) were purchased from Beijing Vital River Laboratory Animal Technology Co., Ltd. Beagle dogs (male: 8.4–9.8 kg, female: 9.1–10.4 kg, 8–12 months old) were purchased from Nanjing chaimen biotechnology Co., Ltd. All animal experiments were carried out according to the protocols approved by Institutional Animal Care and Use Committee (IACUC).

Plasma protein binding assays were conducted by Value pharmaceutical services Co., LTD.

4.1. Synthesis

(2S)-2-(4-((2-Oxocyclopentyl)methyl)phenyl)propanoic acid (S)-1-phenylethan-1-amine (1). To a solution of loxoprofen (9.0 kg, 36.58 mol) in ethyl acetate (70 L) at 27 ± 2 °C in 100 L reaction kettle was added dropwise (*S*)-(−)-1-phenylethylamine (2.07 kg, 17.08 mol). The mixture was stirred for 4–6 h at 23 ± 2 °C and then filtered. The filtrate was discarded and the filter cake was dried at 45–50 °C for 6–8 h in a vacuum drying oven (6–8 Mpa) to give 6.0 kg crude product. The crude product was recrystallized 2 times with a mixed solvent toluene/MeOH to afford compound **1** (3.0 kg, 47.8%).

(2S)-2-(4-((2-Oxocyclopentyl)methyl)phenyl)propanoic acid (2). Compound **1** (1.5 kg), H_2O (6.5 kg), and ethyl acetate (5 L) were added into the reaction kettle with mechanical stirring. The solution was added with 2 N HCl to adjust *pH* 2–3 and stirred for 1h, and then separated. The water layer was then extracted with additional EA (1 L). The extracts were combined, washed with water (6 L) and saturated NaCl solution (1L), dried over Na_2SO_4 for 40 min, and finally evaporated under vacuum ($P \leq -0.05$ Mpa) to give compound **2** (968.5 g, 96.85%).

trans-(2S)-2-(4-((2-Hydroxycyclopentyl)methyl)phenyl)propanoic acid (4). To a solution of compound **2** (920.0 g) in MeOH (1.5 L) and THF (2 L) at 0 °C was added $NaBH_4$ (100 g) over 5 portions. The mixture was allowed to warm to room temperature and stirred overnight. Ethyl acetate and H_2O were added to the mixture and the *pH* was adjusted to 2–3 by 2 N HCl. The organic layer was separated, washed with water (1 L) and saturated NaCl solution (1 L), dried over Na_2SO_4 for 40 min, and evaporated under vacuum ($P \leq -0.05$ Mpa). The crude product was finally purified by flash chromatography (PE/EA = 6:1–4:1) to afford *trans*-alcohol **4** (635.3 g, 68.5%).

(S)-2-(4-(((1S,2R)-2-Acetoxycyclopentyl)methyl)phenyl)propanoic acid (5) *and* ***(S)-2-(4-(((1R,2S)-2-hydroxycyclopentyl)methyl)phenyl)propanoic acid (6, loxoprofenol-SRS).*** Compound **4** (602.9 g, 2.43 mol) was dissolved in ethyl acetate (5 L) and the freshly distilled vinyl acetate (602.9 g, 7.29 mol), Amano PS (90.5 g), and powdered 3 Å MS (90.5 g) in anhydrous toluene (2 L) were added to the solution. The mixture was stirred at 28 °C for 24 h and then filtered. The filtrate was collected and concentrated. The crude product was finally purified by flash chromatography to afford compound **5** and **6.5** (colorless oil, 183.3 g, 26%). ^{1}H NMR (ppm, 500 MHz, DMSO-d_6): δ 12.2316 (s,1H), 7.23015 (d, J = 8.1 Hz, 2H), 7.15145 (d, J = 8.0 Hz, 2H), 4.79345 (s, 1H) 3.6624 (m, 1H), 2.7398 (dd, J = 13.6, 6.5 Hz, 1H), 2.5162 (dd, J = 13.5, 8.7 Hz, 1H),

2.1962–2.2372 (m, 1H), 1.9855–2.0270 (m, 1H), 1.8963 (s, 3H), 1.7353–1.7737(m, 1H), 1.6130–1.6707(m, 2H), 1.5372–1.5863 (m, 1H), 1.38825 (d, J = 7.2 Hz, 3H), 1.2679–1.2989 (m, 1H).

^{13}C NMR (ppm, 125 MHz, DMSO-d_6): δ 175.412, 170.03, 138.89, 138.67, 128.755, 127.208, 79.870, 46.219, 44.390, 38.188, 31.146, 29.165, 21.747, 20.765, 18.471. HRMS (ESI): calcd for $C_{17}H_{22}O_4$, $[M+H]^+$ 291.15909; found, 291.15905, ppm error −0.13.

6 (white solid, 391.9 g, 65%, m.p. 91.3 °C). ^{1}H NMR (ppm, 500 MHz, DMSO-d_6): δ 12.2023 (s, 1H), 7.18595 (d, J = 8.0 Hz, 2H), 7.11955(d, J = 8.0 Hz, 2H), 4.2514 (br, 1H), 3.5868–3.6947 (m, 2H), 2.77705 (dd, J = 13.5, 5.4 Hz, 1H), 2.28675 (dd, J = 13.5, 9.4, 1H), 1.7480–1.9173 (m, 2H), 1.3946–1.6956 (m, 4H), 1.34675 (d, J = 7.1Hz, 3H), 1.1226–1.1336 (m, 1H). ^{13}C NMR (ppm, 125 MHz, DMSO-d_6): δ 175.375, 139.805, 138.313, 128.663, 127.088, 76.358, 48.897, 44.237, 38.444, 33.490, 28.689, 20.940, 18.437. IR (cm^{-1}): 3423.8, 3090.0, 3054.8, 3027.0, 2954.2, 2938.1, 2874.4, 1700.7, 1614.7, 1510.7, 1451.5, 1422.4, 1404.0, 1375.0, 1315.3, 1225.8, 1071.0, 860.7. HRMS (ESI): calcd for $C_{15}H_{20}O_3$, $[M - H]^-$ 247.13397; found, 247.13382, ppm error −0.6. $[\alpha]^{20}$ = +86° (c = 0.15, EtOH).

(S)-2-(4-(((1R,2S)-2-Hydroxycyclopentyl)methyl)phenyl)propanoic acid 2-amino-2-(hydroxymethyl)propane-1,3-diol (HR1405-01). The mixture of compound **6** (391.9 g, 1.58 mol), tromethamine (188.8 g, 1.56 mol) and anhydrous ethanol (1 L) was stirred at 50 °C for 30 min. Activated charcoal (15.7 g) was added to the solution and the mixture was stirred for another 30 min at 50 °C and then filtered. The filter cake was discarded and ethyl acetate (700 mL) was added to the filtrate with the formation of white precipitation. The suspension was stirred for additional 1 h and then filtered to get the filter cake as a white solid, which was dried under vacuum ($P \leq -0.05$ Mpa) to give **HR1405–01** (529.6 g, 92%, m.p. 109.0 °C). ^{1}H NMR (ppm, 500 MHz, DMSO-d_6): δ 7.2021 (d, J = 7.9 Hz, 2H), 7.07445 (d, J = 7.9 Hz, 2H), 3.69835 (q, J = 5.8Hz, 1H), 3.4127–3.4544 (m, 7H), 2.7765 (dd, J = 5.4, 13.5 Hz, 1H), 2.2912 (dd, J = 9.5, 13.5 Hz, 1H), 1.8732–1.9433 (m, 1H), 1.7902–1.8569 (m, 1H), 1.6380–1.7108 (m, 1H), 1.5017–1.6254 (m, 2H), 1.4250–1.4899 (m, 1H), 1.3136 (d, 3H), 1.1401–1.2096 (m, 1H). ^{13}C NMR (ppm, 125 MHz, DMSO-d_6): δ177.923, 141.1542, 138.683, 128.238, 127.236, 76.422, 60.478, 59.834, 49.030, 47.004, 38.570, 33.550, 28.793, 21.044, 19.600. IR (cm^{-1}): 3333.6, 3288.4, 3159.2, 2980.9, 2959.9, 2910.7, 2867.0, 1664.5, 1641.3, 1614.5, 1527.6, 1399.6, 1453.5, 1423.7, 1365.7, 1365.7,1298.9,1285.4, 1196.0, 1076.5, 1047.8. HRMS (ESI$^-$): calcd for $C_{15}H_{20}O_3$, $[M - H]^-$ 247.13397; found, 247.13376, ppm error −0.8. $[\alpha]^{20}$ = +32° (c = 0.1, EtOH).

(S)-2-(4-(((1R,2R)-2-Hydroxycyclopentyl)methyl)phenyl)propanoic acid (PY7). To a solution of **6** (5 g, 20.16 mmol), PPh_3 (12.27 g, 40.32 mmol) and *p*-Nitrobenzoic acid (PNBA, 4.04 g, 24.19 mmol) in THF (80 mL) at 0 °C was added DIAD (8.15 g, 40.32 mmol) dropwise. The mixture was stirred for 4–6 h at 25 °C and then filtered. The filtrate was concentrated under vacuum. The resulting residue was extracted with ethyl acetate (10 mL) three times. The organic layer was washed with water (2 × 50 mL) and brine (50 mL), dried with sodium sulfate, and concentrated to afford **14** (7.5 g) as a colorless oil. Compound **14** and potassium carbonate (7.5 g) were mixed in CH_3OH (40 mL) and stirred at room temperature until the reaction finished. The reaction mixture was next acidified to pH 2 with aq 2 N HCl and extracted with ethyl acetate (50 mL × 3). The organic layer was combined and washed with water (50 mL) and brine (50 mL), dried with sodium sulfate, concentrated, and finally purified by flash chromatography (Hexane/EtOAc) to afford **PY7** (Scheme 3) as a white solid (3.9 g, 78%, m.p. 110.6 °C). ^{1}H NMR (ppm, 500 MHz, DMSO-d_6): δ 12.21 (s, 1H), 7.19 (s, 4H), 4.32 (s, 1H), 3.93 (s, 1H), 3.64 (q, J = 7.1 Hz, 1H), 2.83 (dd, J = 13.5, 7.0 Hz, 1H), 2.50 (dd, J = 13.5, 5.5 Hz, 1H), 1.90–1.82 (m, 1H), 1.76–1.66 (m, 2H), 1.61–1.58 (m, 1H), 1.55–1.51 (m, 1H), 1.49–1.41 (m, 2H), 1.37 (d, J = 7.2 Hz, 2H). ^{13}C NMR (ppm, 125 MHz, DMSO-d_6): δ 175.43, 140.72, 138.16, 128.65, 127.05, 72.21, 47.14, 44.28, 34.59, 34.36, 28.40, 21.31, 18.49. HRMS (ESI-): calcd for $C_{15}H_{20}O_3$, $[M + NH_4]^+$ 266.17507; found, 266.17508, ppm error 0.004. $[\alpha]^{20}$ = +27° (c = 0.15, EtOH).

(S)-2-(4-(((1S,2R)-2-Hydroxycyclopentyl)methyl)phenyl)propanoic acid (PY2). Compound **5** (4.0 g, 13.79 mmol) was dissolved in EtOH and 2 N NaOH was added. The mixture was stirred for approximately 6 h at room temperature. The mixture was filtered and the filtrate was acidified to pH = 2 with aq 2 N HCl and extracted with ethyl acetate (50 mL × 3). The organic layer was combined and washed with water (50 mL) and brine (50 mL), dried with sodium sulfate, concentrated, and finally recrystallized by Hexane/EtOAc to afford **PY2** (Scheme 3) as a white solid (3.0 g, 87.7%, m.p. 108.4 °C). ^{1}H NMR (ppm, 500 MHz, DMSO-d_6): δ 12.21 (s, 1H), 7.21(d, J = 7.9 Hz, 2H), 7.15 (d, J = 7.9 Hz, 2H), 4.54 (s, 1H), 3.70 (q, J = 5.9 Hz, 1H), 3.65 (q, J = 7.1 Hz, 1H), 2.81 (dd, J = 13.6, 5.5 Hz, 1H), 2.32 (dd, J = 13.6, 9.4 Hz, 1H), 1.95–1.88 (m, 1H), 1.86–1.79 (m, 1H), 1.71–1.64 (m, 1H), 1.63–1.50 (m, 2H), 1.49–1.42 (m, 1H), 1.38 (d, J = 7.1 Hz, 3H), 1.15–1.19 (m, 1H). ^{13}C NMR (ppm, 125 MHz, DMSO-d_6): δ 175.39, 139.82, 138.34, 128.68, 127.11, 76.38, 48.92, 44.27, 38.47, 33.51, 28.72, 20.97, 18.47. HRMS (ESI): calcd for $C_{15}H_{20}O_3$, $[M + NH_4]^+$ 266.17507; found, 266.17571, ppm error 2.4. $[\alpha]^{20}$ = +13° (c = 0.15, EtOH).

(S)-2-(4-(((1S,2S)-2-Hydroxycyclopentyl)methyl)phenyl)propanoic acid (PY8). **PY8** was prepared with the method described in the synthesis of **PY7** via Mitsunobu Reactions (Scheme 3). **PY2** (2.0 g) was used as a starting material. **PY8** was finally obtained as a white solid (1.7 g, 85%, m.p. 113.0 °C); ^{1}H NMR (ppm, 500 MHz, DMSO-d_6): δ 12.20 (s, 1H), 7.19 (s, 4H), 4.32 (s, 1H), 3.93 (s, 1H), 3.64 (q, J = 7.1 Hz, 1H), 2.83 (dd, J = 13.6, 7.0 Hz, 1H), 2.50 (dd, J = 13.6, 8.1 Hz, 1H), 1.87–1.85 (m, 1H), 1.72–1.66 (m, 2H), 1.60–1.58 (m, 1H), 1.55–1.51 (m, 1H), 1.49–1.41 (m, 2H), 1.37 (d, J = 7.1 Hz, 3H). ^{13}C NMR (ppm, 125 MHz, DMSO-d_6): δ 175.42, 140.72, 138.15, 128.64, 127.05, 72.21, 47.14, 44.29, 34.59, 34.37, 28.40, 21.31, 18.49. HRMS (ESI): calcd for $C_{15}H_{20}O_3$, $[M + NH_4]^+$ 266.17507; found, 266.17491, ppm error −0.6. $[\alpha]^{20}$ = +66° (c = 0.15, EtOH).

(R)-2-(4-(((1R,2S)-2-Hydroxycyclopentyl)methyl)phenyl)propanoic acid (PY5). **PY5** was prepared with a procedure described in the synthesis of compound **6** (Scheme 2). Loxoprofen (500.0 g, 2.03 mol) and (*R*)-(+)-1-phenylethylamine (115.1 g, 0.95 mol) were used as starting materials. **PY5**: White solid (46.0 g, 9.2%, m.p. 107.9 °C, three steps); ^{1}H NMR (ppm, 500 MHz, DMSO-d_6): δ 12.23 (s, 1H), 7.22 (d, J = 8.1 Hz, 2H), 7.16 (d, J = 8.2 Hz, 2H), 4.55 (s, 1H), 3.71 (q, J = 5.9 Hz, 1H), 3.66 (q, J = 7.1 Hz, 1H), 2.82 (dd, J = 13.6, 8.1 Hz, 1H), 2.33 (dd, J = 13.5, 9.5 Hz, 1H), 1.96–1.89 (m, 1H), 1.87–1.80 (m, 1H), 1.71–1.59 (m, 2H), 1.58–1.51 (m, 1H), 1.50–1.45 (m, 1H), 1.38 (d, J = 7.1 Hz, 3H), 1.21–1.14 (m, 1H). ^{13}C NMR (ppm, 125 MHz, DMSO-d_6): δ 175.45, 139.87, 138.38, 128.73, 127.16, 76.45, 48.98, 44.33, 38.54, 33.57, 28.78, 21.02, 18.50. HRMS (ESI): calcd for $C_{15}H_{20}O_3$, $[M + NH_4]^+$ 266.17507; found, 266.17501, ppm error −0.23. $[\alpha]^{20}$ = −11° (c = 0.15, EtOH).

(R)-2-(4-(((1S,2R)-2-Hydroxycyclopentyl)methyl)phenyl)propanoic acid (PY6). **PY6** was prepared with the method described in the synthesis of **PY2** (Scheme 2) as a white solid (1.42 g, 83%, m.p. 88.8 °C). ^{1}H NMR (ppm, 500 MHz, DMSO-d_6): δ 12.22 (s, 1H), 7.21 (d, J = 8.0 Hz, 2H), 7.15 (d, J = 8.0 Hz, 2H), 4.54 (s, 1H), 3.70 (q, J = 5.9 Hz, 1H), 3.65 (q, J = 7.1 Hz, 1H), 2.81 (dd, J = 13.5, 5.4 Hz, 1H), 2.32 (dd, J = 13.5, 9.5 Hz, 1H), 1.95–1.87 (m, 1H), 1.86–1.79 (m, 1H), 1.70–1.63 (m, 1H), 1.63–1.50 (m, 2H), 1.49–1.43 (m, 1H), 1.38 (d, J = 7.1 Hz, 3H), 1.21–1.14 (m, 1H). ^{13}C NMR (ppm, 125 MHz, DMSO-d_6): δ 175.40, 139.83, 138.36, 128.69, 127.12, 76.39, 48.92, 44.28, 38.48, 33.52, 28.72, 20.97, 18.47. HRMS (ESI): calcd for $C_{15}H_{20}O_3$, $[M + NH_4]^+$ 266.17507; found, 266.17564, ppm error 2.1. $[\alpha]^{20}$ = −80° (c = 0.15, EtOH).

(R)-2-(4-(((1R,2R)-2-Hydroxycyclopentyl)methyl)phenyl)propanoic acid (PY3) *and* ***(R)-2-(4-(((1S,2S)-2-hydroxycyclopentyl)methyl)phenyl)propanoic acid (PY4).*** **PY3** and **PY4** were prepared with the method described in the synthesis of **PY7** as white solids (Scheme 2). **PY3**: white solid (4.9 g, 81.7%, m.p. 104.7 °C); ^{1}H NMR (ppm, 500 MHz, DMSO-d_6): 7.18 (d, J = 7.3 Hz, 2H), 7.13 (d, J = 7.3 Hz, 2H), 3.94 (s, 1H), 3.56 (d, J = 6.5 Hz, 2H), 2.81 (dd, J = 13.2, 6.6 Hz, 1H), 2.47 (dd, J = 13.0, 5.5 Hz, 1H), 1.86 (s, 1H), 1.72 (s, 1H), 1.70 (s, 1H), 1.60–1.57 (m, 1H), 1.55–1.50 (m, 2H), 1.48–1.44 (m, 1H), 1.43–1.39 (m, 1H), 1.33 (d, J = 6.5 Hz, 3H). ^{13}C NMR (ppm, 125 MHz, DMSO-d_6): δ 176.27, 140.02, 139.66, 128.30, 127.10, 72.21, 47.18, 45.50, 34.59, 34.35, 28.39, 21.30, 19.02. HRMS (ESI): calcd for $C_{15}H_{20}O_3$, $[M + NH_4]^+$ 266.17507; found, 266.17503, ppm error −0.15. $[\alpha]^{20} = -47°$ (c = 0.15, EtOH). **PY4**: white solid (0.8 g, 80%, m.p. 111.0 °C); ^{1}H NMR (ppm, 500 MHz, DMSO-d_6): 7.19 (s, 1H), 3.93 (s, 1H), 3.64 (q, J = 7.1 Hz, 1H), 2.83 (dd, J = 13.5, 6.9 Hz, 1H), 2.50 (dd, J = 13.5, 8.0 Hz, 1H), 1.88–1.85 (m, 1H), 1.73–1.70 (m, 2H), 1.58–1.53 (m, 2H), 1.45–1.36 (m, 2H), 1.37 (d, J = 6.5 Hz, 3H). ^{13}C NMR (ppm, 125 MHz, DMSO-d_6): δ 175.47, 140.68, 138.24, 128.63, 127.05, 72.21, 47.14, 44.34, 34.60, 34.37, 28.40, 21.32, 18.52. HRMS (ESI): calcd for $C_{15}H_{20}O_3$, $[M + NH_4]^+$ 266.17507; found, 266.17503, ppm error −0.15. $[\alpha]^{20} = -28°$ (c = 0.15, EtOH).

4.2. Solubility determination

Solubility of **HR1405–01** was determined by the external standard method.

Reference solution: **HR1405–01** (10 mg) was solved in methanol (10 mL) and the solution was then diluted to 100 mL with pre-warmed distilled water (25 °C).

Test solution: **HR1405–01** (500 mg) was added into 1 mL of pre-warmed distilled water (25 °C) and the mixtures were shaken for 30 s every 5 min at 25 °C. After 30 min, the mixture was filtered (0.22 μm PTFE) and the filtrate was collected as the saturated solution.

The reference solution and the test solution were analyzed by high-performance liquid chromatography (Welch Xtimate C18 column, 4.6 mm × 250 mm, 5 μm, temperature: 35 °C, flow rate: 1.0 mL/min, detection wavelength: 220 nm, mobile phase: H_2O: CH_3OH: triethylamine: acetic acid = 400 : 600: 1 : 1), respectively. The solubility of **HR1405–01** was calculated as:

$$C_{test} = \frac{A_{test}}{A_{ref}} \cdot C_{ref}$$

C_{test}: concentration of test solution
C_{ref}: concentration of reference solution
A_{test}: peak area of test solution
A_{ref}: peak area of reference solution

4.3. Animal models

All animals were treated following the Guide for Care and Use of Laboratory Animals, approved by the Animal Experimentation Ethics Committee of Jiangsu Center for Safety Evaluation of Drugs (Nanjing, China, Permit number LL-20190508-01). Male Sprague-Dawley rats (180–220 g, 2.5–3 months old, approved number: SCXK2016-0006) and ICR mice (18–22 g, approved number: SCXK2016-0003) were purchased from Beijing Vital River Laboratory Animal Technology Co., Ltd. and used in the anti-inflammatory and analgesic experiments, pharmacokinetic study, plasma protein binding assay, and toxicity test. Animals were housed in clear stainless steel cages (5 rats/cage) and maintained in a temperature (20–26 °C) and humidity (40–70%) controlled room, under a 12 h light/dark cycle, with *ad libitum* access to food and water. All animals were allowed to adapt to laboratory conditions for at least 7 days before the initiation of any experiment. An observer conducted all the behavioral assays. Beagle dogs (approved number: SCXK2016-0001) were purchased from Beijing Marshall Biotechnology Co., Ltd and used in the pharmacokinetic study, plasma protein binding assay, and toxicity test. Young New Zealand White rabbits (approved number: SCXK2019-0005) were purchased from the Laifu farms in Pukou District, Nanjing, and used in the local tolerance study.

4.4. Conversion of HR1405–01 to PY2-PY8

HR1405–01 injection was administered intravenously to rats (3 males and 3 females) and Beagle dogs (5 males and 5 females) at the dosage of 3 mg/kg, respectively. Blood samples were drawn at 5 min, 30 min, 1 h, 2 h, 4 h, 8 h, and 24 h post dose in a microfuge tube pretreated with EDTA. Clear supernatant plasma was separated from blood after the centrifugation (2500 xg, 4 °C, 5 min). Samples were kept at −20 °C until further analysis. The extractions of plasma samples were vortexed for 30 s, and then transformed to 96-well plates and vortexed for another 3 min with methanol. The samples were then subjected to centrifuge at 3200 xg at 4 °C for 5 min. The supernatants were transformed to another 96-well plate and dried under a gentle nitrogen flow at 35 °C. The residues were dissolved in methanol and subjected to ultra-high-performance liquid chromatography (UHPLC, SHIMATSU UFLC 30-AD, Japan) with a CHIRALPAK column (250 mm × 4.6 mm with a particle size of 5 μm) for separation. The column temperature was 40 °C, and the sample injection volume was 5 μL. The mobile phase consisted of a mixture of methanol and 0.1% formic acid (40: 60, v/v) in a running time of 120 min at a flow rate of 1 mL/min. The qualitative analysis of **HR1405–01** to **PY2-PY8** was carried out with mass spectrometry (ESI+, API 5500, Applied Biosystems) under multiple reaction monitoring.

4.5. Pharmacokinetic study

Pharmacokinetic studies were carried out with the Beagle dog and Sprague-Dawley rat. In each animal model, the dosages were set as 0.2 mg/kg, 0.8 mg/kg and 3 mg/kg. Each group contained six animals (3 males and 3 females). The concentrations of **HR1405–01** in the plasma of the animals were evaluated with LC-MS/MS. EDTA-K_2 was used as an anticoagulant. The pharmacokinetic parameters were calculated using non-compartmental analysis with WinNonLin(version 7.0, Pharsight)

4.6. Plasma protein binding assays

Plasma protein binding assays of **HR1405–01** in plasma of CD-1 mouse, Sprague-Dawley rat, Beagle dog, Cynomolgus monkey, and human were performed with rapid equillibrium device (RED, Thermo Scientific). The equilibrium time was firstly determined with human plasma (sample chamber) and phosphate buffer saline (PBS) (buffer chamber). Human plasma containing 3000 ng/ml of **HR1405–01** was added into the sample chamber in RED and then incubated in a water bath at 37 °C for 1 h, 2 h, 4 h, 6 h, or 8 h. The concentration of **HR1405–01** in each buffer chamber was then tested with LC-MS/MS (MRM). The time-concentration curve was next drawn and the best equilibrium time was then determined as 6 h. The plasma samples (CD-1 mouse serum, Sprague-Dawley rat serum, Beagle dog serum, Cynomolgus monkey serum, and human serum) containing the indicated concentrations of **HR1405–01**

(600 ng/ml, 3000 ng/ml, or 15,000 ng/ml) were added into sample chambers in RED and incubated in a water bath at 37 °C for 6 h. The concentrations of **HR1405–01** in the buffer chambers were next tested with LC-MS/MS (MRM). The binding rate of plasma protein was calculated as:

Binding rate of plasma protein (%) = $[(C_{plasma}\text{-}C_{buffer})/C_{plasma}] \times 100$.

A tritium-labeled Taxol (2000 ng/ml) was used as a positive control. C_{plasma} represents the concentration of **HR1405–01** in plasma. C_{buffer} represents the concentration of **HR1405–01** in PBS buffer.

4.7. Formalin test

Formalin solution (1.2%, 100 μL) was subcutaneously injected into the plantar surface of the right hind paw of the rat (intraplantar, i.pl.). Three levels of stereotyped behaviors (3 points: licking/biting and shaking of the injected paw; 2 points: flinching of the injected paw; 1 point: limping) were considered as a nociceptive response and were registered from 10 min to 60 min after injection. Three levels of behaviors were recorded at the same time and the final results were expressed as the sum of three nociceptive responses: the numbers and scores of evoked licking/biting and flinching/shaking and limping. Two periods were considered: an early phase covered from the time immediately after the injection to 10 min later and which corresponds to acute nociceptive pain; and a late phase from 10 to 30 min after formalin injection that corresponds to inflammatory pain.

4.8. Model of 0.6% carrageenan-induced arthritic inflammation

Acute inflammation was induced in male Sprague-Dawley rats by injecting freshly prepared 0.6% (W/V) of carrageenan in 0.9% sterile saline into the left hind paw (0.1 mL/rat). Ten minutes after injection, all of the rats were used for hind paw swelling measurement and behavioral tests. Hind paw edema was evaluated by measuring hind paw swelling.

4.9. The writhing test

The writhing test was selected as a model of acute visceral pain. All animals were acclimatized to the laboratory environment. Each mouse was injected (i.p.) with 0.2 ml of 0.6% acetic acid. The number of abdominal writhes was counted during a 15-min period, starting right after the administration of the acetic acid solution. A writhe was defined as a contraction of the abdominal muscles followed by body elongation and hind limbs' extension. Drugs and their vehicles were given 15 min before the injection of acetic acid. Anti-nociceptive activity (reduction in writhes) was expressed as a percent inhibition effect that was calculated by the following equation: (mean writhes in control group-mean writhes in drug(s) treated group)/mean of writhes in the control group. Ten animals were used at each dose level to determine the ED_{50} value.

4.10. Paw pressure test

The anti-hyperalgesic activity was assessed by a modified 'paw pressure' test. The rat was placed with its hind paws on two force transducer platforms of the apparatus (Hugo Sachs Elektronik, March-Hugstetten, Germany) and pushed slowly and smoothly downwards. The pressure was applied until one of the paws received force that exceeded the trigger level set at 100 g. At this point, an audible click by the apparatus was heard and measurement was stopped automatically. The rat used its noninflamed paw as the weight-bearing limb in an attempt to spare the inflamed paw. Thereby, agents capable of reducing the difference between the forces (df) applied to the noninflamed vs. the inflamed paw were recognized as possessing anti-hyperalgesic activity. The forces applied to the paws were read on the display, and the differences in force were expressed as the percent of anti-hyperalgesic activity (% AH) and calculated according to the following formula:

AH%= (mean force (g) applied to the noninflamed paw-mean force (g) applied on inflamed paw)/mean force (g) applied to the noninflamed paw.

To induce inflammation, 0.1 ml/rat of 4% (w/v) kaolin (Sinopharm Chemical Reagent Co., Ltd) suspension injection was given and 1 h later, 0.1 ml/rat of 1% (w/v) carrageenan (SIGMA) was injected into the right hind paw in overnight fasted rats. To determine mechanical hyperalgesia, paw withdrawal threshold (g) was measured using an analgesic meter 2.5 h after modeling.

4.11. Local tolerance study

Young New Zealand White rabbits of either sex, weighting 2.5–3 kg, were used in the experiment. The animals were housed individually in cages with observation for seven days and trained to be familiar with the handling procedures during the last two days before the start of the experiment. Five animals were set as a group. The skin was shaved 24 h before the injection. The left ear of each animal received an intravenous injection of 10 mg/kg/day (volume: 1 ml/kg) for seven days and the right ear was given 0.9% saline at the same volume as a negative control. After the last injection, animals were observed for another three days (three animals) or fourteen days (two animals) and then necropsied. The injected muscle was isolated using dissection and the injection site was localized over a light cabinet. Macroscopic damages were examined by slicing the muscle. The samples bearing the representative lesions were excised and immersed in 10% neutral buffered formalin for 24 h. Paraffin sections were then prepared with the fixed tissues, stained with H&E (Haematoxylin and Eosin), and finally investigated with an optical microscopy equipped with a digital camera.

4.12. Repeated administration toxicity test

Repeated administration toxicity tests were performed with Beagle dogs and Sprague-Dawley rats for four weeks. Animals were treated with **HR1405–01** every day at the dosages of 1 mg/kg, 3 mg/kg, or 10 mg/kg for four weeks. The physiological saline (0.9% NaCl) was used as a vehicle for intravenous administration. After four weeks of convalescence, hematological analyses were performed with the blood of animals.

4.13. Study of plasma concentration-time curves

Healthy people were divided into five groups and each group contained 10 people (5 male and 5 female). Each group was treated with **HR1405–01** intravenously at the dosages of 10 mg, 20 mg, 40 mg, 80 mg, or 120 mg. The blood samples were collected at 0 h (before treatment), 0.17 h, 0.33 h, 0.5 h, 0.67 h, 0.83 h, 1.0 h, 1.25 h, 1.50 h, 2.0 h, 2.5 h, 3.0 h, 4.0 h, 6.0 h and 8.0 h. The concentrations of **HR1405–01** in the blood samples were determined by LCMS/MS. The experiments have been approved by the Ethics Committee at Sir Run Run Hospital, Nanjing Medical University (approved number: 2021-GCP-003).

Author contributions

The manuscript was written through the contributions of all authors. All authors have reviewed the final version of the manuscript and approved it for submission to the journal.

Declaration of competing interest

The authors declare that they have no known competing financial interests or personal relationships that could have appeared to influence the work reported in this paper.

Acknowledgments

The work was supported by the National Natural Science Foundation of China (81930099, 82130102, 81773664), the Natural Science Foundation of Jiangsu Province (BK20212011), "Double First-Class" University project (CPU2018GY47, CPU2018GF10), 111 Project from the Ministry of Education of China and the State Administration of Foreign Expert Affairs of China (No. 111-2-07, B17047), the Open Project of State Key Laboratory of Natural Medicines (No. SKLNMZZ202017), and Construction Project of Jiangsu Engineering Research Center (BM2019213).

Appendix A. Supplementary data

Supplementary data to this article can be found online at https://doi.org/10.1016/j.ejmech.2022.114258.

References

[1] D.A. Kujubu, B.S. Fletcher, B.C. Varnum, R.W. Lim, H.R. Herschman, TIS10, a phorbol ester tumor promoter-inducible mRNA from Swiss 3T3 cells, encodes a novel prostaglandin synthase/cyclooxygenase homologue, J. Biol. Chem. 266 (1991) 12866–12872.
[2] W.L. Xie, J.G. Chipman, D.L. Robertson, R.L. Erikson, D.L. Simmons, Expression of a mitogen-responsive gene encoding prostaglandin synthase is regulated by mRNA splicing, Proc. Natl. Acad. Sci. U. S. A. 88 (1991) 2692–2696.
[3] J.R. Vane, Y.S. Bakhle, R.M. Botting, Cyclooxygenases 1 and 2, Annu. Rev. Pharmacol. Toxicol. 38 (1998) 97–120.
[4] J.K. Gierse, S.D. Hauser, D.P. Creely, C. Koboldt, S.H. Rangwala, P.C. Isakson, K. Seibert, Expression and selective inhibition of the constitutive and inducible forms of human cyclo-oxygenase, Biochem. J. 305 (Pt 2) (1995) 479–484.
[5] M. Noguchi, A. Kimoto, J.K. Gierse, M.C. Walker, B.S. Zweifel, K. Nozaki, M. Sasamata, Enzymologic and pharmacologic profile of loxoprofen sodium and its metabolites, Biol. Pharm. Bull. 28 (2005) 2075–2079.
[6] F.E. Silverstein, G. Faich, J.L. Goldstein, L.S. Simon, T. Pincus, A. Whelton, R. Makuch, G. Eisen, N.M. Agrawal, W.F. Stenson, A.M. Burr, W.W. Zhao, J.D. Kent, J.B. Lefkowith, K.M. Verburg, G.S. Geis, Gastrointestinal toxicity with celecoxib vs nonsteroidal anti-inflammatory drugs for osteoarthritis and rheumatoid arthritis: the CLASS study: a randomized controlled trial. Celecoxib Long-term Arthritis Safety Study, JAMA 284 (2000) 1247–1255.
[7] C. Bombardier, L. Laine, A. Reicin, D. Shapiro, R. Burgos-Vargas, B. Davis, R. Day, M.B. Ferraz, C.J. Hawkey, M.C. Hochberg, T.K. Kvien, T.J. Schnitzer, V.S. Group, Comparison of upper gastrointestinal toxicity of rofecoxib and naproxen in patients with rheumatoid arthritis, VIGOR Study Group, N. Engl. J. Med. 343 (2000) 1520–1528, 1522 pp. following 1528.
[8] G.A. FitzGerald, C. Patrono, The coxibs, selective inhibitors of cyclooxygenase-2, N. Engl. J. Med. 345 (2001) 433–442.
[9] R. Caporali, C. Montecucco, Cardiovascular effects of coxibs, Lupus 14 (2005) 785–788.
[10] J.M. Brophy, Cardiovascular effects of cyclooxygenase-2 inhibitors, Curr. Opin. Gastroenterol. 23 (2007) 617–624.
[11] C. Patrono, Cardiovascular effects of cyclooxygenase-2 inhibitors: a mechanistic and clinical perspective, Br. J. Clin. Pharmacol. 82 (2016) 957–964.
[12] H. Krum, D. Liew, J. Aw, S. Haas, Cardiovascular effects of selective cyclooxygenase-2 inhibitors, Expert Rev. Cardiovasc Ther. 2 (2004) 265–270.
[13] L.J. Scott, Intravenous ibuprofen: in adults for pain and fever, Drugs 72 (2012) 1099–1109.
[14] R. Bhuniya, S. Nanda, Asymmetric synthesis of the active form of loxoprofen and its analogue, Tetrahedron Asymmetry 22 (2011) 1125–1132.
[15] T.S. Koo, D.H. Kim, S.H. Ahn, K.P. Kim, I.W. Kim, S.Y. Seo, Y.G. Suh, D.D. Kim, C.K. Shim, S.J. Chung, Comparison of pharmacokinetics of loxoprofen and its active metabolites after an intravenous, intramuscular, and oral administration of loxoprofen in rats: evidence for extrahepatic metabolism, J. Pharm. Sci.-Us 94 (2005) 2187–2197.
[16] D. Riendeau, M. Salem, A. Styhler, M. Ouellet, J.A. Mancini, C.S. Li, Evaluation of loxoprofen and its alcohol metabolites for potency and selectivity of inhibition of cyclooxygenase-2, Bioorg. Med. Chem. Lett 14 (2004) 1201–1203.
[17] M. Sugimoto, Y. Toda, M. Hori, A. Mitani, T. Ichihara, S. Sekine, S. Kaku, N. Otsuka, H. Matsumoto, Topical anti-inflammatory and analgesic effects of multiple applications of *S*(+)-Flurbiprofen plaster (SFPP) in a rat adjuvant-induced arthritis model, Drug Dev. Res. 77 (2016) 206–211.
[18] T. Mandai, T. Yamakawa, An efficient synthesis of (2*S*)-2-[4-((1R, 2*S*)-2-hydroxycyclopentylmethyl)phenyl]propionic acid, Synlett 6 (2000) 862–864.
[19] R. Tanikaga, A. Morita, Lipase-mediated diastereoselective and enantioselective acetylations of 3-substituted cyclohexanols, Tetrahedron Lett 39 (1998) 635–638.
[20] O.O. Kolodiazhna, A.O. Kolodiazhna, O.I. Kolodiazhnyi, Enzymatic preparation of (1S,2R)- and (1R,2S)-stereoisomers of 2-halocycloalkanols, Tetrahedron Asymmetry 24 (2013) 37–42.
[21] N.M. Davies, N.M. Skjodt, Choosing the right nonsteroidal anti-inflammatory drug for the right patient: a pharmacokinetic approach, Clin. Pharmacokinet. 38 (2000) 377–392.